Available online at www.sciencedirect.com
SCIENCE DIRECT®
Journal of Magnetic Resonance 165 (2003) 128–136
JMR Journal of Magnetic Resonance
www.elsevier.com/locate/jmr

Electronic *g*-factor measurement from ENDOR-induced EPR patterns: malonic acid and guanine hydrochloride dihydrate

Junseog Kang, Sibel Tokdemir, Jun Shao, and William H. Nelson*

Department of Physics and Astronomy, Georgia State University, Atlanta, GA 30303, USA

Received 2 June 2003; revised 14 July 2003

Abstract

Measurement of electronic *g*-factors ($\overrightarrow{\overrightarrow{g}}$) from radicals in irradiated organic crystals is generally difficult because the overall EPR pattern is usually the composite of several components, e.g., from multiple radicals and from multiple magnetic sites. However, when an ENDOR line is fully resolved, the method of ENDOR-induced EPR (EI-EPR, or EIE) in principle permits identification of the EPR pattern from the individual component yielding the line. To examine this method as an approach useful for measuring $\overrightarrow{\overrightarrow{g}}$, we used it to measure those of known radicals in two different crystal systems. First, to verify correspondence of the EIE and EPR sufficient for using EIE patterns to extract $\overrightarrow{\overrightarrow{g}}$, we used both EIE and EPR to measure $\overrightarrow{\overrightarrow{g}}$ of $\cdot CH(COOH)_2$ from irradiated crystals of malonic acid. Then, to illustrate the procedure applied to a system giving a more complex EPR pattern, we used EIE to measure $\overrightarrow{\overrightarrow{g}}$ of the O6-protonated anion radical of guanine in irradiated guanine $\cdot$ HCl $\cdot$ $2H_2O$ crystals. EPR results from the malonic acid radical are $g_{max} = 2.00374(2)$, $g_{mid} = 2.00331(2)$, and $g_{min} = 2.00234(3)$; EIE results from the same radical are $g_{max} = 2.00375(2)$, $g_{mid} = 2.00334(2)$, and $g_{min} = 2.00238(2)$, where numbers in parentheses indicate statistical uncertainties in the respective least significant digits. In addition, eigenvectors from the two sets of measurements agree to approximately 1°. Results from the guanine radical are $g_{max} = 2.00490(2)$, $g_{mid} = 2.00318(4)$, and $g_{min} = 2.00218(4)$. (The uncertainties should reliably indicate relative accuracy, while absolute accuracy is within ± 0.0002 as indicated by simultaneous measurement of Cr^{3+} in MgO.)

Keywords: Malonic acid; Guanine $\cdot$ HCl $\cdot$ $2H_2O$; *g*-Tensor; EI-EPR

1. Introduction

As indicated by the spin Hamiltonian in Eq. (1) below, $\overrightarrow{\overrightarrow{g}}$ is perhaps the most basic magnetic characteristic of a paramagnetic species [1]. Although orientation-dependent as $\overrightarrow{\overrightarrow{g}}$, its

$$\mathcal{H} = \beta \overrightarrow{B} \cdot \overrightarrow{\overrightarrow{g}} \cdot \overrightarrow{S} \tag{1}$$

effective value (g_{eff}) determines the magnetic field position at which the paramagnetic resonance occurs according to the "resonance" condition in Eq. (2) below (in the form appropriate for $S = 1/2$). Since Planck's constant (h) and the Bohr magneton (β) are fundamental

$$h\nu_{mw} = g_{eff}\beta B_R \tag{2}$$

constants, measurement of g_{eff} requires combined measurement of the operating microwave frequency (ν_{mw}) and the magnetic field position at which the resonance occurs (B_R) according to Eq. (3). For EPR spectra where hyperfine interactions create a multi-line pattern, the equivalent of B_R is B_c, the center or midpoint of the spectrum (to first order in $A/h\nu$; see the discussion on malonic acid below)

$$g_{eff} = \frac{h\nu_{mw}}{\beta B_R}. \tag{3}$$

Irradiation of organic solids generally leads to formation of multiple radical species, thereby creating an EPR pattern that is the composite of several individual components. Measurement of g_{eff} for each species directly from the EPR is difficult under these circumstances due to the overlapping patterns and consequent uncertain location of the midpoint for each component. Further increasing the difficulty are the multiple patterns

* Corresponding author. Fax: 1-404-651-1427.
E-mail address: wnelson@gsu.edu (W.H. Nelson).

1090-7807/$ - see front matter © 2003 Elsevier Inc. All rights reserved.
doi:10.1016/S1090-7807(03)00256-8

created by the "site splitting" commonly present in EPR spectra from crystals. In addition, components of the $\overrightarrow{\overrightarrow{g}}$ for radicals in irradiated organic crystals typically vary only slightly from the free-electron value (ca. ± 0.005) making $\overrightarrow{\overrightarrow{g}}$ information much less useful than hyperfine information in providing evidence helpful for identifying radicals. Partly due to their lower "identification value" and partly due to the measurement difficulty, g-values are much less frequently included among the magnetic parameters reported from studies of radiation-induced radicals. In fact, reports from our laboratory mainly have given hyperfine couplings obtained with the ENDOR method and rarely have reported $\overrightarrow{\overrightarrow{g}}$ information.

However, successful simulation of EPR spectra expected from randomly oriented radicals can depend strongly on $\overrightarrow{\overrightarrow{g}}$ information [2–4]. This is true for the K-band (~24 GHz) microwave frequencies used in our laboratory, for the Q-band (~35 GHz) frequencies used in many laboratories, and particularly true for the much higher frequencies (up to 300+ GHz) used in an increasing number of laboratories [4]. The extent to which this is important is demonstrated in the concluding discussion with spectra simulated from the malonic acid results.

Because $\overrightarrow{\overrightarrow{g}}$ information is important to effective simulations of spectra expected for known radicals, we chose to investigate the ENDOR-induced EPR (EI-EPR, or EIE) [5,6], method as a means of extracting $\overrightarrow{\overrightarrow{g}}$ from overlapping EPR spectra. The potential for doing so with EIE is based on the much higher resolution of ENDOR spectra in comparison to EPR. With ENDOR, the individual lines are completely resolved in most cases. The EIE method, accomplished by fixing the RF generator to an ENDOR peak and sweeping the magnetic field, provides the magnetic profile of the ENDOR response. In the usual case, this magnetic profile corresponds to the EPR extent of only the radical from which the ENDOR arises. (In some cases, intra- or inter-molecular cross-relaxation may suppress the ENDOR effect for a portion of the field range and distort the EIE pattern.) In principle, therefore, g_{eff} of a specific radical species (or magnetic site) can be measured simply by finding the magnetic field value at the center of the corresponding EIE pattern.

We took a two-step approach in this investigation. The first was to ensure that EIE patterns could represent EPR spectra with fidelity sufficient for extracting g_{eff}. For this purpose, we chose the radical $\cdot CH(COOH)_2$ in irradiated crystals of malonic acid. Malonic acid was attractive for several reasons: the crystals are triclinic so there would be no magnetic site splitting; it is a well-studied system where it is known that the crystals can be heat-treated after irradiation so that only the $\cdot CH(COOH)_2$ radical remains [7]; the EPR spectrum from this radical is well-resolved at many orientations, making it straightforward to identify the center of the pattern. These characteristics permit measurement of g_{eff} from both the EPR and EIE patterns as is necessary to validate the EIE method.

The second step was to apply the EIE method to a system giving a more complex EPR pattern. For this case we chose the radical previously identified as the O6-protonated guanine anion in guanine $\cdot$ HCl $\cdot$ $2H_2O$ (guanine hydrochloride dihydrate, or Gd) crystals [8]. The Gd crystals are monoclinic and exhibit magnetic site splitting; in addition, under the conditions where the O6-protonated anion radical exists, two other radicals coexist. Thus, the Gd system presents examples of all the factors described above as complications for g_{eff} measurement.

2. Experimental

Malonic acid crystallizes with a triclinic unit cell [9,10]; it was possible to grow large crystals by slowly evaporating aqueous solutions of the commercially available compound. Suitable crystals were irradiated to a total dose of approximately 50 kGy at room temperature with X-rays from a tungsten-target tube operating at 55 kV from a constant-potential supply. Heat treatment at 60 °C for 12–15 h following the irradiation essentially eliminated all radicals except $\cdot CH(COOH)_2$ [7]. Guanine $\cdot$ HCl $\cdot$ $2H_2O$ crystallizes with a monoclinic unit cell [11]; suitable crystals grew from sealed solutions on a hotplate as previously described [8]. These were irradiated at 150 K, also to ca. 50 kGy. After irradiation, the crystals were annealed at 180 K for approximately 15 min to allow all O6-protonated anion radicals to adopt the most stable conformation described in the previous study [8]. Data from malonic acid were collected by rotation of annealed crystals (at room temperature) about the a^*, b^*, and $\langle 10\bar{2}\rangle^*$ axes, and data from Gd were collected by rotation of annealed crystals (cooled to 150 K) about b, c^*, and $\langle 01\bar{1}\rangle^*$. All EPR spectra were recorded as second-derivatives, and ENDOR spectra as first-derivatives, using previously described instrumentation [8].

To record EIE patterns, it is necessary to scan the magnetic field with the ENDOR frequency fixed on a peak (in our case this is a first-derivative peak). However, the exact frequency of an ENDOR line is a function of the free proton frequency, described to first order according to $\nu = |\nu_n \pm a/2|$. Thus, the ENDOR frequency is a function of the field value, and maintaining the ENDOR frequency at the peak position requires a field-dependent adjustment of the frequency. Our procedure is to monitor the high-frequency ENDOR line while scanning the frequency simultaneously with the field according to:

$$\nu = \nu_0 + (B - B_0) \times (g_n \beta_n / h), \tag{4}$$

where v_0 and B_0 are the RF and magnetic field values for the initial ENDOR spectrum; v and B are the instantaneous values during the scan; g_n and β_n are the appropriate nuclear values, and h is Planck's constant.

At the outset, our goal was to measure g_{eff} ($\sim$2.0) to $\pm$0.0001; doing so requires overall measurement capability of 0.5×10^{-4} or 5 parts in 10^5. At the K-band frequency of ca. 24.0 GHz, this requires frequency measurement to $\pm$1.2 MHz. This is well within the measurement capability of modern microwave frequency counters; moreover, the frequency stability of our spectrometer during a scan is better than 1 part in 10^6. Thus, frequency measurement capabilities and spectrometer stability did not limit measurement of g_{eff}, making the main challenge that of measuring B_c, the midpoint of the EPR (or EIE) pattern, to 5 parts in 10^5. For the approximate 0.85 T (8500 G) field value (for B_c at 24.0 GHz when $g_{\text{eff}} = 2.0$), this required identifying and measuring B_c to $\pm$0.425 G.

The microwave frequency was measured with Hewlett–Packard counters (5343A or 5351A). The magnetic field was set and swept by direct computer control of a Bruker BH-15 unit, while the magnetic field value at the beginning and end of the scan was read from an NMR gaussmeter (Bruker ER 035M) with the probe centered in the magnet gap and located as close to the sample cavity as possible ($\sim$30 mm in front). Direct measurement indicated the field values at the NMR and sample positions were related by $(B_{\text{sample}} - B_{\text{NMR}}) = 0.42$ G over the full range of the scans. Actual field values were calculated from the NMR measurements by linearly rescaling the raw values established by the BH-15 set points.

To provide a continuous check on this relationship, each EPR spectrum also includes that of Cr^{3+} ions in MgO from a sample located at the wall of the cylindrical microwave resonator. Previous studies of the Cr^{3+}:MgO system reported g_e values of 1.9800 ± 0.0006 [12], 1.9797 (no uncertainty quoted) [13], 1.9798 ± 0.0001 [14,15], and 1.9810 ± 0.0006 [16]. Our results from more than 50 measurements, made as described above, gave the value $g_e = 1.97971 \pm 0.00001$. However, this level of precision indicates the high degree of consistency among the data in our experiments but does not account for systematic errors, e.g., from placement of the NMR probe relative to the reference sample. Nevertheless, the strong correspondence between our value and those reported previously makes it reasonable to state that $g_e = 1.9797 \pm 0.0002$ for Cr^{3+} ions in MgO.

Results were extracted from the angular-dependence data by use of the program MAGRES [17]. Recent modifications to the program incorporate non-linear least-squares techniques to provide a refinement of the results by adjustment of the polar and intersection angles of the datasets to minimize the weighted χ^2 for the complete set of data. The program also provides standard error estimates for the eigenvalues and eigenvectors derived from the data.

Peak positions for the ESR and EIE data were measured using Origin 6.1 with the following procedure. After reading the spectrum file (recorded at 0.1 G resolution) into Origin, the spectrum was treated with 8- to 64-point FFT smoothing, with the specific choice depending on the degree of noise in the raw spectrum. The peak of the smoothed pattern was then located by use of a routine written in the Origin scripting language. Specifically, the routine fits a parabola to 25 points surrounding an initial position located visually (by a mouse click) in the vicinity of the peak; following the mouse click, the position of the parabola is iterated automatically until convergence. Since the apex of the converged parabola indicates the peak, the measurement incorporates interpolation and provides results as though the data were continuous.

3. Results from malonic acid

Fig. 1 shows representative EPR, ENDOR, and EIE patterns from a malonic acid crystal. These indicate the degree to which only the $\cdot CH(COOH)_2$ radical is present in the heat-treated crystals. Fig. 2a shows the angular dependence of g_{eff} measured from the EPR in three planes while Fig. 2b shows that of g_{eff} measured from

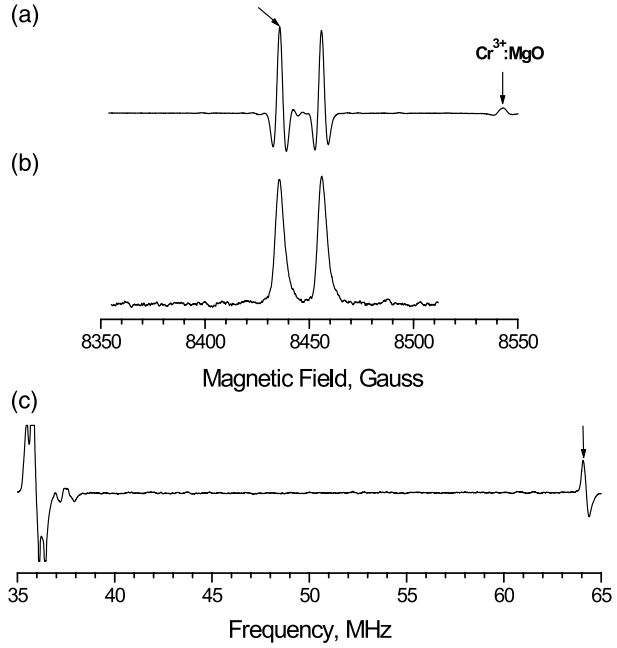

Fig. 1. (a) EPR (second-derivative) from malonic acid; (b) EIE from the ENDOR line (first derivative) indicated by the arrow in (c); (c) ENDOR with the field set on the EPR at the position indicated by the arrow in (a). The magnetic field is at a position in the *ac* crystallographic plane 30° from $\langle a \rangle$.

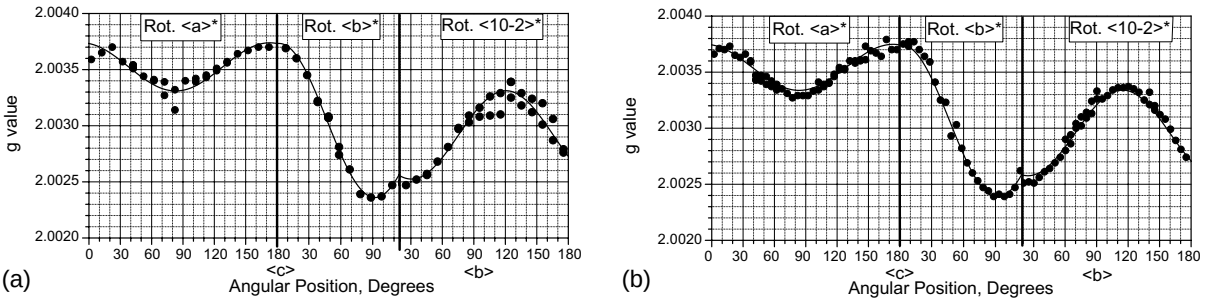

Fig. 2. (a) Angular dependence of the g-values measured from malonic acid EPR for rotation of crystals about three axes as indicated. Note that all three rotation axes are parallel to reciprocal lattice vectors as indicated by the "*." (b) Angular dependence of the g-values measured from EIE patterns for the same crystals and rotations as (a). In both figures, filled circles indicate actual data while the continuous lines were calculated from the tensors in Table 1. Also in both figures, the x-axis scale for the Rot. $\langle b\rangle^*$ set does not extend to 180° and that for the Rot. $\langle 10\bar{2}\rangle^*$ set does not begin at 0°. Instead, the respective x-axes are truncated at the positions where the planes of data intersect.

the EIE patterns in three planes. That the results are virtually identical is reinforced by the values extracted from the data, listed in Table 1.

For ease of comparison, the results reported in Table 1 are presented in a system defined by the hyperfine coupling tensor: $\boldsymbol{X}$ is the direction of $A_{\min}$, $\boldsymbol{Y}$ is the direction of $A_{\max}$, and $\boldsymbol{Z}$ is the direction of A_{mid}. These directions are related to the malonic acid ·CH group as shown in Scheme 1. Although the hyperfine coupling itself is not the focus of this study, it should be noted that the eigenvalues are virtually the same as those reported by Sagstuen et al. [18] for a previous study at room temperature; as well, the eigenvalues correspond well to those reported by McCalley and Kwiram [19] for crystals cooled to 4.2 K. It should also be noted that the results reported here for $\overrightarrow{\overrightarrow{g}}$ correspond to those in the original study by McConnell et al. [7] according to:

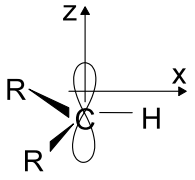

Scheme 1. Relation of coordinate axes to the ·CH group of the malonic acid radical.

Table 1
Results from malonic acid

Eigenvalue	Eigenvector[a]		
	$\langle \boldsymbol{X}\rangle$	$\langle \boldsymbol{Y}\rangle$	$\langle \boldsymbol{Z}\rangle$
$\overrightarrow{\overrightarrow{g}}$ from EPR			
2.00374(2)	−0.102(30)	0.991(6)	−0.092(50)
2.00331(2)	0.990(1)	0.093(20)	−0.103(30)
2.00234(3)	0.093(20)	0.101(50)	0.991(6)
$\overrightarrow{\overrightarrow{g}}$ from EIE			
2.00375(2)	−0.092(20)	0.992(9)	−0.085(40)
2.00334(2)	0.979(2)	0.075(20)	−0.192(20)
2.00238(2)	0.184(20)	0.101(40)	0.978(4)
$\overrightarrow{\overrightarrow{A}}_1$ from ENDOR (MHz)			
−90.98(3)	0.0000	1.0000	0.0000
−57.05(4)	0.0000	0.0000	1.0000
−28.51(5)	1.0000	0.0000	0.0000
$\overrightarrow{\overrightarrow{A}}_2$ from ENDOR (MHz): (Ref. [19])			
9.66(2)	0.5225	0.7734	0.3591
3.61(2)	−0.8429	0.4050	0.3541
3.18(3)	0.1284	−0.4877	0.8635
Experimental $\langle a^*b'c\rangle$ system in the molecule-based XYZ system			
$\hat{\mathbf{a}}^*$	0.1219	0.0719	0.9899
$\hat{\mathbf{b}}'$	−0.9923	0.0311	0.1199
$\hat{\mathbf{c}}$	0.0222	0.9969	−0.0752

[a] The molecule-based system is defined by the hyperfine tensor as follows: $\boldsymbol{X}$ is the direction of $A_{\min}$, $\boldsymbol{Y}$ is the direction of $A_{\max}$, and $\boldsymbol{Z}$ is the direction of A_{mid}.

$g_x = 2.00331$ (vs. 2.0033), $g_y = 2.00374$ (vs. 2.0035), $g_z = 2.00234$ (vs. 2.0026). (The two studies have opposite definitions of the z and x directions; those given are from this study.)

Eigenvalues are listed to six significant figures in Table 1; this reflects the overall rms deviation of the datasets (0.00006 and 0.00005 for the EPR and EIE sets, respectively) and the large number of data points (96 and 139 for EPR and EIE, respectively). While we believe this is an accurate indication of the overall results, the ± 0.0002 uncertainty quoted above for g of the Cr^{3+}:MgO reference unfortunately makes this sample incapable of providing a double-check on the absolute accuracy of the results. However, for spectrum simulation applications, the relative accuracy of the eigenvalues and the accuracy of the eigenvectors are more important since they directly affect the simulated lineshape. For the eigenvectors, the statistical analysis indicates a worst-case deviation of approximately $\pm 5°$ from the directions listed.

A final point regarding $\overrightarrow{g}$ for malonic acid is that use of the field value at the midpoint of the EPR pattern for calculating g_{eff} is accurate only to first order in $A/h\nu$. However, the error at $g \cong 2$ in doing so is of the order $\frac{1}{2}(A/h\nu)^2$ [1]; for $A/h \cong 100\,\text{MHz}$ and $\nu \cong 24\,000\,\text{MHz}$, this evaluates to an error of $\sim 8.7 \times 10^{-6}$ which is negligible in comparison to the statistical uncertainties.

4. Results from guanine · HCl · $2H_2O$

Previous study has shown that X-irradiation of Gd crystals cooled to 150 K or lower leads to at least three stabilized radical species [8]. One species was identified as the result of electron addition followed by protonation of the parent molecule at O6 and is referred to as the "O6-protonated anion." Scheme 2 below shows the N7-protonated cationic form of guanine as it exists in Gd crystals and Scheme 3 shows the O6-protonated anion (equivalent to O6 hydrogenation). Hyperfine couplings in Scheme 3 are well-known from studies of Gd and other crystals where the guanine parent is as shown by Scheme 2 [20–22].

Fig. 3d shows an EPR pattern from Gd, Fig. 3a shows ENDOR from the central region of the EPR, and the remaining patterns of Fig. 3 show EIE from ENDOR lines as indicated. This figure illustrates several properties of EIE. For example, patterns 3e and f are sharp and similar enough to associate them with one

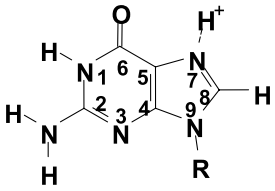

Scheme 2.

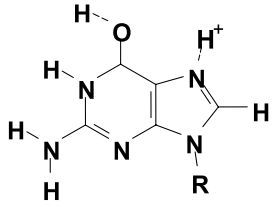

Scheme 3.

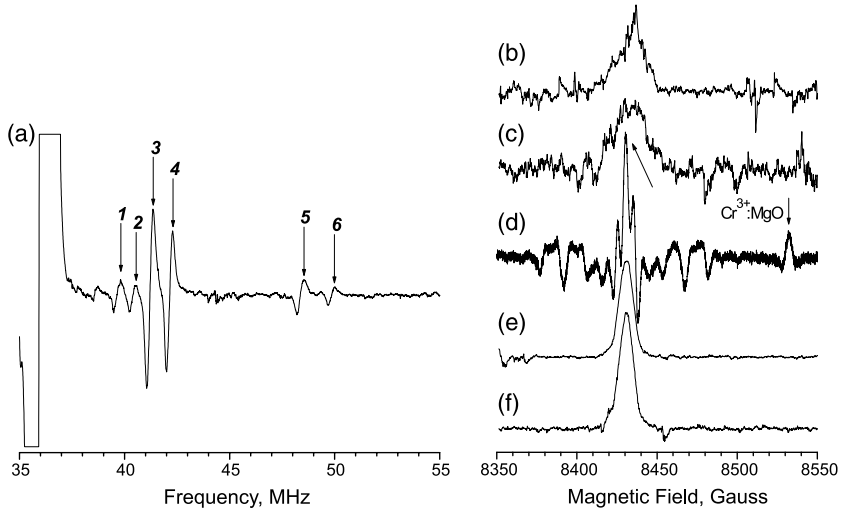

Fig. 3. (a) ENDOR from the central peak of the second-derivative EPR shown in (d); (b) EIE from peak 5 of (a); (c) EIE from peak 1 of (a); (d) EPR; (e) EIE from peak 3 of (a); (f) EIE from peak 4 of (a). Patterns (b) and (c) are from one magnetically distinct site (I) while those of (e) and (f) are from the other site (II). Line 6 of (a) is from another radical and line 2 is from a third interaction of the anion radical. These patterns were obtained with the magnetic field $\sim 25°$ from $\langle a \rangle$ with rotation about the $\langle 01\bar{1} \rangle^*$ axis.

magnetic site while patterns 3b and c are broader and exhibit much lower signal-to-noise ratio, similarities associating them with the other magnetic site. In addition, for both magnetic sites, in principle there should be three EIE patterns: one from each of three hyperfine couplings, to HN1, HN7, and HC8. (At the magnetic field orientation for the spectra of Fig. 3, ENDOR lines from one of the interactions were not clearly resolved.) Thus, a radical with multiple hyperfine interactions provides the opportunity for multiple g_{eff} measurements at one position thereby enhancing the statistical significance of the results. For the results reported below, all available data were used.

Also, the EIE patterns in Fig. 3 illustrate the challenges for using EIE to extract g_{eff} values within ± 0.0001, requiring measurement of B_c to ± 0.42 G. Specifically, the sharp and symmetric patterns of 3e and f yield peak values different by only 0.09 G following FFT smoothing. On the other hand, the detail shown in Fig. 4 demonstrates that the patterns of Fig. 3b and c are much poorer in quality and yield peak values different by ca. 1.6 G after smoothing. Worse, the smoothed version of pattern 3b shows clear asymmetry, a property making the peak of the pattern no longer representative of the pattern's center. Because EIE patterns often are noisy and asymmetric, we explored several moment-based methods for selecting patterns of high quality for the dataset [23]. For example, the position of the peak and the position about which the first moment is zero will be the same for a symmetric pattern; the difference between these is a measure of asymmetry therefore. In addition, we considered methods other than peak measurement for objectively identifying the start, end, and midpoint of a pattern. In the end, however, for the results described here, we used exclusively the method of measuring the peak of the FFT-smoothed pattern.

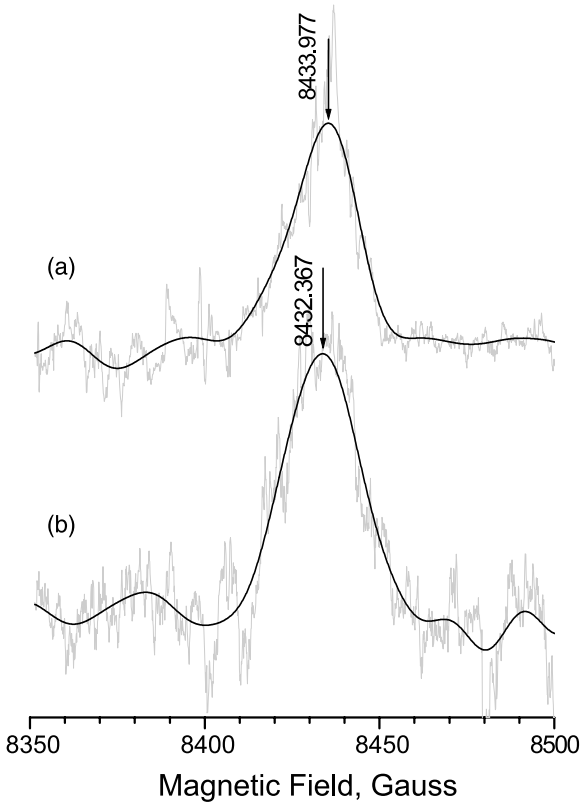

Fig. 4. Detail of EIE patterns in Figs. 3b and c. (a) The lightly shaded pattern is the same as Fig. 3b while the solid line is the result of FFT smoothing. The arrow indicates the "peak" and apparent "center" of the pattern. (b) Similar representation of Fig. 3c. Note the asymmetry apparent in (a) and the difference in peak positions.

Fig. 5 shows the angular dependence of the measurements and Table 2 shows the tensors derived from the data. Also for ease of comparison, all results from Gd are expressed in a coordinate system based on the structure of the undamaged molecule: $\boldsymbol{Z}$ is the normal to the least-squares plane through the ring atoms, $\boldsymbol{X}$ is perpendicular to $\boldsymbol{Z}$ and the C4–C5 bond, and $\boldsymbol{Y}$ is perpendicular to both $\boldsymbol{Z}$ and $\boldsymbol{X}$. Scheme 4 illustrates this system. Although the scatter in the data is higher with Gd than malonic acid (rms deviations of 0.0002 for Gd vs. 0.00005 for the malonic acid EIE dataset), the large number of data points (153) provided sufficient statistical averaging that the uncertainty in the eigenvalues is in the 5th decimal place. As above, the uncertainties quoted are reliable for the relative values of the $\overrightarrow{\overrightarrow{g}}$ components while the absolute values may be uncertain to ± 0.0002 subject to undetected systematic errors in measuring the absolute magnetic field value at the sample.

5. Summary and conclusions

The primary objective of measuring $\overrightarrow{\overrightarrow{g}}$ of a radical is to provide this magnetic parameter for cases where it is

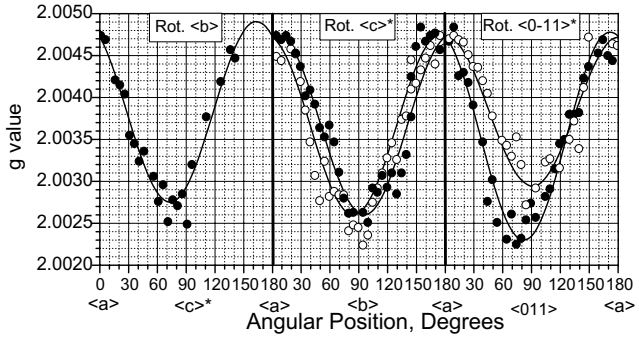

Fig. 5. Angular dependence of the g-values measured from rotation of Gd crystals about three axes as indicated. Filled and open circles indicate the actual data while the continuous curve was calculated from the results in Table 2. In the center and right-hand panels, filled and open circles indicate data from the two magnetically distinct sites of the crystals. The sites are related by the direction-dependent portion of the monoclinic symmetry transformation: $(x, y, z) \rightarrow (x, -y, z)$.

Table 2
Results from guanine · HCl · $2H_2O$

Eigenvalue[b]	Eigenvector[a,b]		
	$\langle X \rangle$	$\langle Y \rangle$	$\langle Z \rangle$
$\overrightarrow{\overrightarrow{g}}$			
2.00490(2)	0.625(0)	0.780(1)	0.039(13)
2.00318(4)	0.775(1)	−0.625(1)	0.095(22)
2.00218(4)	−0.094(3)	0.029(3)	0.995(23)
$\overrightarrow{\overrightarrow{A}}$ from HN1: (Ref. [8])			
−15.90(2)	0.401(2)	−0.916(20)	−0.025(20)
−10.80(2)	−0.002(20)	−0.028(9)	−0.999(40)
−0.60(2)	0.916(20)	0.400(40)	0.012(4)
$\overrightarrow{\overrightarrow{A}}$ from HN7: (Ref. [8])			
−12.60(2)	0.999(2)	0.032(20)	−0.000(20)
−10.60(2)	0.000(20)	0.010(9)	0.999(40)
−1.10(2)	0.032(20)	−0.999(40)	0.001(4)
$\overrightarrow{\overrightarrow{A}}$ from HC8: (Ref. [8])			
−33.50(2)	0.078(2)	−0.996(20)	0.042(20)
−23.40(2)	−0.030(20)	0.040(9)	0.999(40)
−10.00(2)	−0.997(20)	−0.079(40)	−0.027(4)
Experimental $\langle a^* bc \rangle$ system in the molecule-based XYZ system			
$\langle a^* \rangle$	0.7453	0.5940	0.3029
$\langle b \rangle$	−0.6030	0.4066	0.6863
$\langle c \rangle$	0.2845	−0.6942	0.6612

[a] The molecule-based coordinate system is defined as follows: $\boldsymbol{Z}$ is normal to the least-squares plane through the ring atoms (N1, C2, ..., C8, and N9); $\boldsymbol{X}$ is normal to $\boldsymbol{Z}$ and the C4–C5 bond; $\boldsymbol{Y}$ is normal to $\boldsymbol{Z}$ and $\boldsymbol{X}$. Vectors for the second magnetic site are related to these by the direction-dependent portion of the monoclinic cell symmetry transformation: $(x, y, z) \rightarrow (x, -y, z)$.

[b] The numbers in parentheses represent uncertainties in the last digit(s).

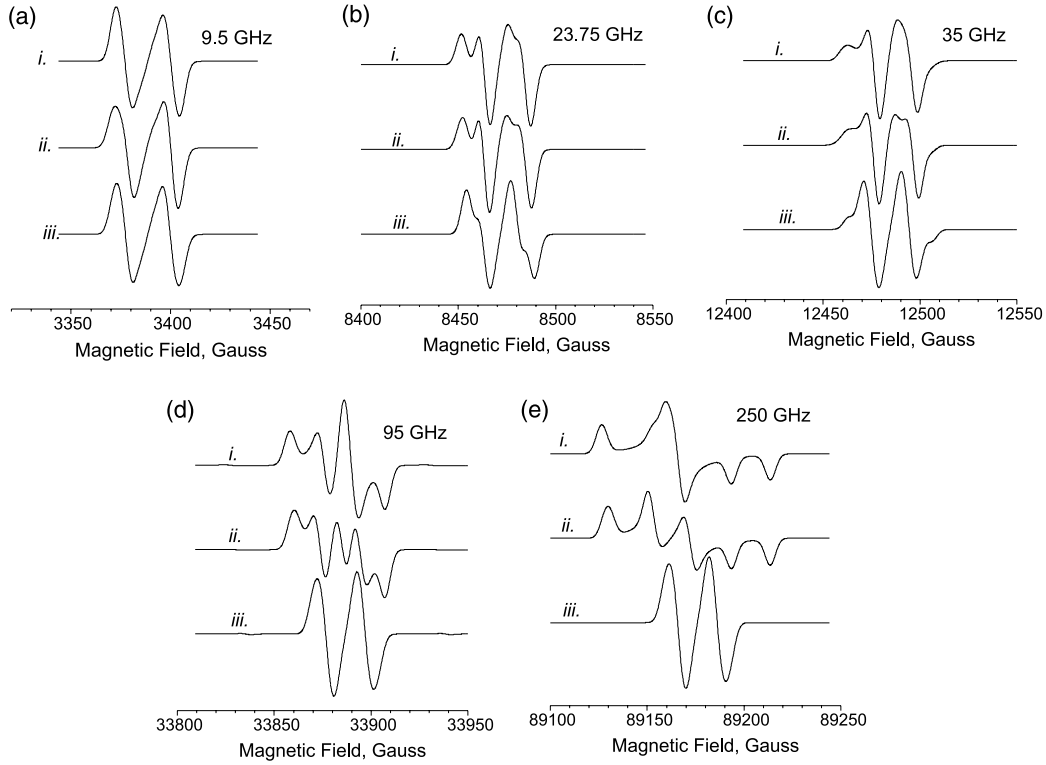

Fig. 6. Powder lineshape simulations for malonic acid. (a–e) Lineshapes for the microwave frequencies indicated as follows: (i) lineshape using $\overrightarrow{\overrightarrow{g}}$ and $\overrightarrow{\overrightarrow{A}}$ as described in Table 1; (ii) lineshape with $\overrightarrow{\overrightarrow{A}}$ from Table 1 and $\overrightarrow{\overrightarrow{g}}$ rotated about Z by 45°; (iii) lineshape with $\overrightarrow{\overrightarrow{A}}$ from Table 1 and isotropic g.

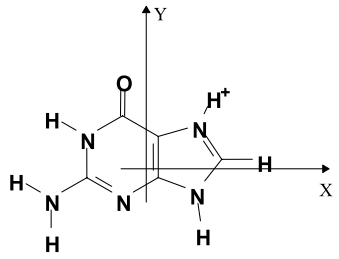

Scheme 4. Illustration of the molecule-based coordinate system used for Gd. ***Z*** is normal to the molecular plane.

necessary to simulate the EPR spectrum, e.g., for randomly oriented radicals (or "powder" samples). Fig. 6 illustrates the effect of g anisotropy with the spectrum of a randomly oriented distribution of the $\cdot CH(COOH)_2$ radicals. From comparison of Figs. 6a–e, it is clear that g-anisotropy affects the lineshape to a degree increasing with microwave frequency. Moreover, it is clear from the patterns at higher frequencies that the lineshape is affected in a noticeable—and quantifiable—way when the relative orientation between $\overrightarrow{\overrightarrow{g}}$ and $\overrightarrow{\overrightarrow{A}}$ is changed. This means that accurate lineshape analysis requires accurate knowledge of the relative orientation of $\overrightarrow{\overrightarrow{g}}$ and $\overrightarrow{\overrightarrow{A}}$. As an example from Fig. 6b, ignoring the g-anisotropy at K-band leads to the r^2-value [24] between Figs. 6b(i) and (iii) of 0.77; Figs. 6b(i) and (ii) show that rotation of $\overrightarrow{\overrightarrow{g}}$ by 45° about Z yields $r^2 = 0.97$.

In conclusion, therefore, the malonic acid results demonstrate that peaks in EIE patterns represent those of the EPR spectrum well enough that $\overrightarrow{\overrightarrow{g}}$ measured from either are virtually identical. Application of the EIE method to Gd permitted measurement of $\overrightarrow{\overrightarrow{g}}$ for the O6-protonated anion radical in a system with multiple radicals and multiple magnetic sites where there is very little chance for success from EPR alone. Moreover, the large number of data points available from the EIE approach permits $\overrightarrow{\overrightarrow{g}}$ measurement with uncertainty an order of magnitude lower than usual with EPR. Consequently, the EIE method is clearly valuable for $\overrightarrow{\overrightarrow{g}}$ measurement.

Acknowledgments

This work was supported by PHS Grant CA36810 awarded by NIH/NCI, and was supported in part by the Research Program Enhancement (RPE) fund of Georgia State University. In addition, the authors gratefully acknowledge a gift of the Cr^{3+}:MgO sample from Dr. Chester Alexander, and assistance from Dr. Tomasz Wasowicz in collecting the malonic acid data.

References

[1] N.M. Atherton, Principles of Electron Spin Resonance, Ellis Horwood, London, 1993.
[2] W. Bernhard, A. Patrzalek, ESR characteristics of one-electron-reduced thymine in monomer, oligomer, and polymer derivatives, Radiat. Res. 117 (1989) 379–394.
[3] M.D. Sevilla, D. Becker, M. Yan, S.R. Summerfield, Relative abundances of primary ion radicals in γ-irradiated DNA: cytosine vs. thymine anions and guanine vs. adenine cations, J. Phys. Chem. 95 (1991) 3409–3415.
[4] B. Weiland, J. Hüttermann, J. van Tol, Primary free radical formation in randomly oriented DNA: EPR spectroscopy at 245 GHz, Acta Chem. Scand. 51 (1997) 585–592.
[5] J.S. Hyde, ENDOR of free radicals in solution, J. Chem. Phys. 43 (1965) 1806–1818.
[6] R.J. Cook, Electron nuclear double resonance at 35 000 Mc/s, J. Sci. Instr. 43 (1966) 548–553.
[7] H.M. McConnell, C. Heller, T. Cole, R.W. Fessenden, Radiation damage in organic crystals. I. $CH(COOH)_2$ in malonic acid, J. Am. Chem. Soc. 82 (1960) 766–775.
[8] W.H. Nelson, E.O. Hole, E. Sagstuen, D.M. Close, ESR/ENDOR study of guanine · HCl · $2H_2O$ X-irradiated at 20 K, Int. J. Radiat. Biol. 54 (1988) 963–986.
[9] J.A. Goedkoop, C.H. McGillavry, The crystal structure of malonic acid, Acta Cryst. 10 (1957) 125–127.
[10] N.R. Jagannathan, S.S. Rajan, E. Subramanian, Refinement of the crystal structure of malonic acid, $C_3H_4O_4$, J. Chem. Crystallogr. 24 (1994) 75–78.
[11] J. Iball, H.R. Wilson, The crystal structure of guanine hydrochloride dihydrate, Proc. R. Soc. (Lond.) A 288 (1965) 418–429.
[12] J.E. Wertz, P. Auzins, Crystal vacancy evidence from electron spin resonance, Phys. Rev. 106 (1957) 484–488.
[13] G.A. Woonton, G.L. Dyer, On the hyperfine structure of trivalent chromium in a cubic environment, Can. J. Phys. 45 (1967) 2265–2279.
[14] W.M. Walsh Jr., J. Jeener, N. Bloembergen, Temperature-dependent crystal field and hyperfine interactions, Phys. Rev. 139 (1965) A1338–A1350.
[15] W.-C. Zheng, S.-Y. Wu, Investigations of the temperature dependence of the electron paramagnetic resonance g-factor for the MgO:Cr^{3+} crystal, J. Phys.: Condens. Matter 8 (1996) 4539–4544.
[16] W. Low, Paramagnetic resonance and optical absorption spectra of Cr^{3+} in MgO, Phys. Rev. 105 (1957) 801–805.
[17] W.H. Nelson, Estimation of errors in eigenvectors and eigenvalues from magnetic resonance results using linear data-fitting techniques, J. Magn. Reson. 38 (1980) 71–78.
[18] E. Sagstuen, A. Lund, Y. Itagaki, J. Maruani, Weakly coupled proton interactions in the malonic acid radical: single crystal ENDOR analysis and EPR simulation at microwave saturation, J. Phys. Chem. A 104 (2000) 6362–6371.
[19] R.C. McCalley, A.L. Kwiram, ENDOR studies of the radicals in malonic acid single crystals, J. Phys. Chem. 97 (1993) 2888–2903.
[20] E. Sagstuen, E.O. Hole, W.H. Nelson, D.M. Close, ESR/ENDOR study of guanosine-5′-monophosphate (free acid) single crystals X-irradiated at 10 K, Radiat. Res. 116 (1988) 196–209.
[21] D.M. Close, W.H. Nelson, E. Sagstuen, Radical formation in X-irradiated single crystals of guanine hydrochloride monohydrate. Part II. ESR and ENDOR in the range 10–77 K, Radiat. Res. 112 (1987) 283–301.
[22] E.O. Hole, E. Sagstuen, W.H. Nelson, D.M. Close, Radiation damage to guanine hydrobromide monohydrate. Solid state

ESR and ENDOR between 8 and 295 K, Radiat. Res. 125 (1991) 119–128.

[23] J. Shao, The use of field-swept ENDOR for *g*-factor measurement of purine and pyrimidine radicals, Ph.D. Dissertation, Georgia State University, 1994 (Univ. Microfilms Int., DA9503503).

[24] M.Z. Heydari, E. Malinen, E.O. Hole, E. Sagstuen, Alanine radicals, Part 2: the composite polycrystalline alanine EPR spectrum studied by ENDOR, thermal annealing, and spectrum simulation, J. Phys. Chem. A 106 (2002) 8971–8977.